

Fig. 3. Time of flight spectra of $m/e = 32$ from ozone photodissociation at 193 nm detected at $\Theta = 20^\circ$. Upper: ionization energy 17 eV, middle: 13.5 eV, lower: 10.5 eV. TOF peaks are labeled consistent with results from Ref. 2. D. Stranges, X. Yang, J. D. Chesko and A. G. Suits, *J. Chem. Phys.* **102** (15), 6067 (1995).

3. Photochemistry

3.1. Dimethyl Sulfoxide

Among the compelling advantages of PI-based photodissociation studies using photofragment translational spectroscopy (PTS) is the ability to study complex systems and complex dissociation processes in great detail. This is well illustrated in the recent study⁷ of the photodissociation of dimethyl sulfoxide (DMSO). Earlier investigations based on state-resolved resonance enhanced multiphoton ionization (REMPI) probe of the methyl radical in conjunction with laser induced fluorescence (LIF) studies on

the SO product,⁸ concluded that the dissociation mechanism for DMSO at 193 nm was a concerted one and which both methyl radicals departed simultaneously. This conclusion was based on the observation of internally cold methyl radical products and the REMPI studies. Recent studies on the Chemical Dynamics Beamline, however, using the tunable VUV probe have found the dissociation mechanisms to be considerably more complex than previously supposed. Figure 4 shows time-of-flight (TOF) spectra for the CD₃SO product from dissociation of deuterated DMSO at angles of 12° and 22.5°. The observation of this intermediate, made possible through the use of the tunable, soft ionization, demonstrates conclusively that this dissociation is stepwise rather than concerted. Furthermore, as is apparent in the TOF spectra and in the corresponding translational energy distributions shown in Fig. 5, this product arises from two distinct channels. One with considerable translational energy release, greater than 25 kcal/mol, and the other peaking at much lower translational energies, around 8 kcal/mol. The TOF spectra for the corresponding methyl radicals, shown in Fig. 6, mass 18 for CD₃⁺, are momentum-matched to the sulfonyl intermediate shown in Fig. 4. It is worth noting that these very high signal-to-noise

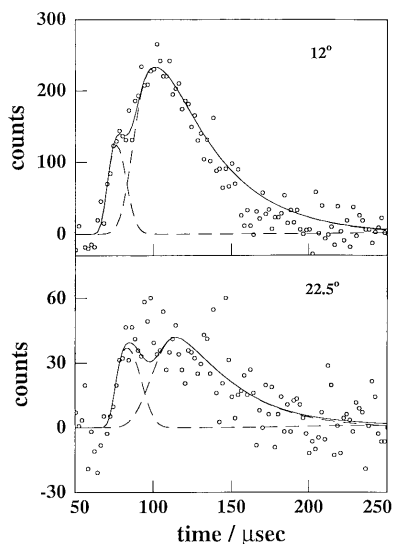


Fig. 4. TOF spectra for m/e 66 (CD₃SO⁺) at source angles of 12° and 22.5°. The forward convolution fit contains two contributions representing the fast and slow channels for reaction discussed in the text and fitted with the $P(E_T)$ s in Fig. 5.

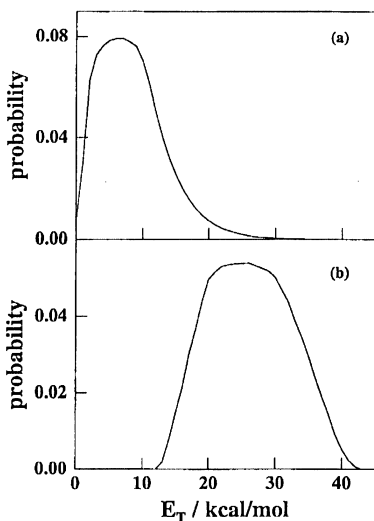


Fig. 5. The center-of-mass translational energy distribution used to fit the sulfonyl radicals in Fig. 4, showing fast and slow contributions ascribed to dissociation on excited and ground state potential surfaces, respectively.

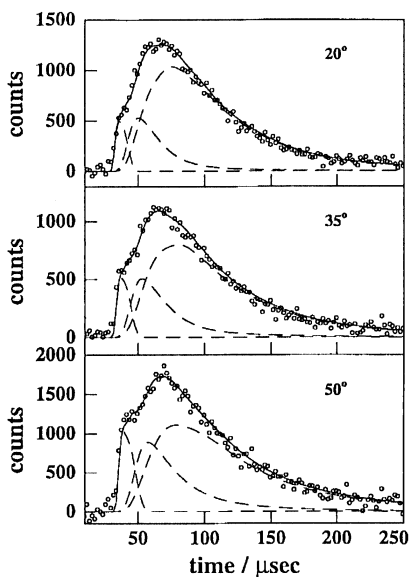


Fig. 6. The TOF spectra for CD_3^+ at the indicated angles, showing three contributions as described in the text.

(S/N) time-of-flight spectra are recorded at m/e 18, a peak in the water background for conventional mass spectrometers. The use of the tunable VUV allows for probing CD_3 well below the ionization potential of water, resulting in greatly reduced background at these masses. In addition to the primary contributions shown in the methyl radical TOF spectra, there are also contributions from secondary decomposition of the intermediates. In fact, by fitting the TOF spectra for the methyl and the intermediates simultaneously, one can extract directly the fraction of intermediates that undergo secondary decomposition to give a second methyl radical. This is shown in Fig. 7 where the shaded area represents the fraction of the primary sulfonyl intermediates that subsequently decompose to give an additional methyl radical and an SO molecule. In addition, the SO product could be momentum-matched to the methyl from secondary decomposition of the sulfonyl intermediates shown in Fig. 5(a).

The results for DMSO-h6 shows some fascinating differences from those for the perdeuterated molecule. Most significantly, no CH_3SO intermediates were observed. It is believed that the inability to observe these arises from several factors. Foremost among these is that a larger fraction of the CH_3SO intermediates in the slow primary dissociation process undergo secondary decomposition. In addition, it appears that the fast channel is less important in DMSO-h6 than in DMSO-d6. In fact, the largest problem arises from the difficulty in resolving the mass 62 and mass 63 contributions, that

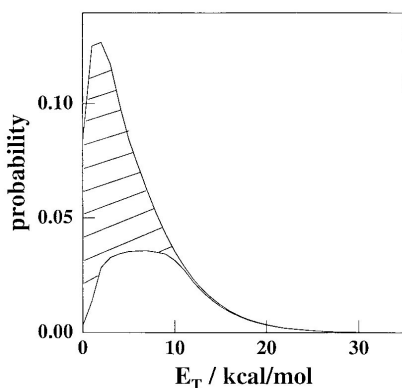


Fig. 7. The center-of-mass translational energy distributions derived from fitting both primary methyl and sulfonyl radical products. The shaded area is the difference between fits to the methyl and sulfonyl contributions, and represents the primary c.m. translation energy distribution for sulfonyl intermediates that undergo secondary C-S bond cleavage.

the onset of dissociative ionization processes for some channels, making near background-free TOF measurements possible. Second is the knowledge of the probe photon energy. Even in the case where dissociative ionization is possible, its presence or absence is used to provide some insight into the internal energy in the products. Finally, the universal nature of the detection scheme allows for essential momentum-matching to exclude multi-photon and secondary decomposition processes and to allow for quantitative assignment of the branching into various channels.

3.2. Substituted Ethylenes

Another class of systems that shows clearly the power of tunable undulator radiation in conjunction with PTS is a collaborative study of the photodissociation dynamics of substituted ethylenes⁹ involving the Brookhaven group of North and Hall, with the Berkeley team of Blank, Suits and Lee. Ethylene and the substitute ethylenes are a widely studied class of molecules that exhibit a strong $\pi^* \leftarrow \pi$ transition in the vicinity of 190 nm. We will first consider the dissociation of acrylonitrile or cyanoethylene and contrast its photodissociation dynamics with those of the more widely studied vinyl chloride system.

3.2.1. Acrylonitrile

Results for acrylonitrile dissociation at 193 nm obtained on the Chemical Dynamics Beamline show four distinct dissociation channels, and the results are consistent with the occurrence of all of these on the ground state potential energy surface following internal conversion from the excited state. Hydrogen elimination results in the C_3H_2N radical, m/e 52. TOF spectra for this product are shown in Fig. 9 along with the result of a forward convolution simulation. The energy distribution used to fit these spectra is shown in the Fig. 10 and compared with a statistical prior distribution. In addition to measuring the TOF spectra, one can also record a low resolution photoionization efficiency (PIE) spectrum for this radical simply by tuning the undulator gap. This is shown in Fig. 11 at a source angle of 7.5° . The observed photoionization onsets depend on a complex combination of factors since the detected products contain unknown amounts of internal energy, and the influence of this internal energy on the photoionization threshold is not clear. Based on the energy release, the radicals that are probed in